bradscholars

Compact Dielectric Resonator Antenna with Band-Notched Characteristics for Ultra-Wideband Applications

Item Type	Article
Authors	Majeed, Asmaa H.;Abdullah, Abdulkareem S.;Sayidmarie, Khalil H.;Abd-Alhameed, Raed;Elmegri, Fauzi
Citation	Majeed AH, Abdullah AS, Sayidmarie KH et al (2015) Compact Dielectric Resonator Antenna with Band-Notched Characteristics for Ultra-Wideband Applications. Progress in Electromagnetics Research C. 57: 137–148.
DOI	https://doi.org/10.2528/pierc15022102
Rights	© 2015 PIER-C and The Electromagnetics Academy. Reproduced in accordance with the publisher's self-archiving policy.
Download date	2025-02-19 10:07:25
Link to Item	http://hdl.handle.net/10454/7884

Compact Dielectric Resonator Antenna with Band-Notched Characteristics for Ultra-Wideband Applications

**Asmaa H. Majeed[1, 2], Abdulkareem S. Abdullah[1], Khalil H. Sayidmarie[3],
Raed A. Abd-Alhameed[2, *], Fauzi Elmegri[2], and James M. Noras[2]**

Abstract—In this paper, a compact dielectric resonator antenna (DRA) with band-notched characteristics for ultra-wideband applications is presented. A comprehensive parametric study was carried out using CST Microwave Studio Suite TM 2011 to analyze and optimize the characteristics of the proposed antenna. Three shapes for the coupling slot were investigated. Simulation results show that the proposed DRA had a -10 dB impedance bandwidth of 23% from 9.97 GHz to 12.558 GHz, and a maximum gain of 7.23 dBi. The antenna had a notched band centered at 10.57 GHz, which increased the reflection coefficient by 23.5 dB, and reduced the gain by 6.12 dB. The optimized designs were verified by experimental tests on fabricated samples.

1. INTRODUCTION

The interest in dielectric resonator antennas (DRAs) for a variety of wireless communications systems has grown in the last few years [1–8]. Dielectric resonators (DRs) are fabricated from low-loss dielectric materials, for which the resonant frequency is predominantly a function of size, shape and permittivity. DRs offer the advantages of small size, low profile light weight, and high radiation efficiency, which make them attractive for many wireless applications [9–13]. A recent trend for DRA design has been in meeting Ultra-Wideband (UWB) specifications, and high data-rate wireless LANs, as well as applications in radar and imaging systems [14–17]. Various bandwidth enhancement techniques have been applied within DRAs using different excitation mechanisms to excite several modes covering wider bandwidths.

In the last decade, there has been a growing need for broadband antennas that can satisfy the entire frequency range of future UWB systems with a reasonable performance. Recently, UWB has been used widely in applications such as radar, telemetry, navigation, biomedical systems, mobile satellite communications, the direct broadcast system (DBS), global positioning systems (GPS), and remote sensing. The design of an appropriate antenna for these systems is one of the most important current challenges [18].

Since the frequency range of a UWB system is very wide, many other systems can coexist and may cause interference. Therefore, certain frequencies in the UWB range need to be rejected leading to a need for band-notched antennas. The main problem of band rejection design is the difficulty of controlling the bandwidth of the notched band in a limited antenna space. Moreover, while adequate band rejection is highly desirable, the performance of the antenna should remain essentially the same for the rest of the band.

Recently, a number of UWB antennas with band-notched properties were presented where various methods have been used to achieve the band notching. Examples of approaches used are;

- inverted U-shaped slots and H-shaped slot [19],
- U-shaped slots and E-shaped slot [20],
- folded stripline slot and a pair of inverted L-shaped slots [21],
- half wavelength C-shaped slot in the patch and two half-wavelength stepped impedance resonators around the feed-line [22],
- three open-ended quarter-wavelength slots [23],
- L-shaped two slots and open-loop resonator [24], and
- stepped impedance resonator-defected ground structure (SIR-DGS) and fork-shaped stubs [25].

The performances of band-notching techniques used have been recently compared in [26]. A similar comparison included the use of fractal shapes to control the notched band frequency center and width [27]. In a recent publication, good band-notched performance is achieved by using high permittivity and low dielectric loss substrates, and inserting quarter-wavelength horizontal/vertical stubs or alternatively embedding quarter-wavelength open-ended slots within the feed line [28]. Gain suppressions of up to 15 dB were obtained.

In the present paper, a compact, $(30 \times 25)\,\text{mm}^2$ DRA with aperture coupling and a $50\,\Omega$ microstrip feed line is presented. The performances of elliptical, rectangular and C-slot apertures are investigated, and then the band-notching was implemented using a U-shaped slot in the feed line. The results reported in this paper are obtained using the CST software package [29], which is used in the design and parametric studies of the investigated antennas. The optimized designed antennas were fabricated and tested experimentally for verification.

2. ANTENNA GEOMETRY OF THE ELLIPTICAL SLOT FED CYLINDRICAL DRA

Figure 1 shows the geometry of the proposed dielectric resonator antenna fed by an elliptical slot. It was printed on a 0.8 mm thick Rogers TMM4$^{\text{tm}}$ substrate with relative permittivity $\varepsilon_r = 4.5$ and dielectric loss tangent of 0.017. The ground plane was printed on the substrate with dimensions of $(30 \times 25)\,\text{mm}^2$ small enough to fit on circuit boards for many wireless communication applications. The DRA cylinder had diameter $D = 6\,\text{mm}$, height $h = 9\,\text{mm}$, and was made of alumina material with $\varepsilon_r = 9.4$. The DRA position was slightly offset from the center point of the slot along the feed line. An elliptical shape slot with major slot radius s_l and minor slot radius s_w was etched on the ground plane as a feeding mechanism for coupling and bandwidth enhancement. A microstrip feed line with length $l_f = 22.5\,\text{mm}$ and width $l_w = 1.5\,\text{mm}$ was used to couple the input signal to the DRA through the elliptical slot, connected to a $50\,\Omega$ coaxial SMA connector as a feeding port.

(a)   (b)
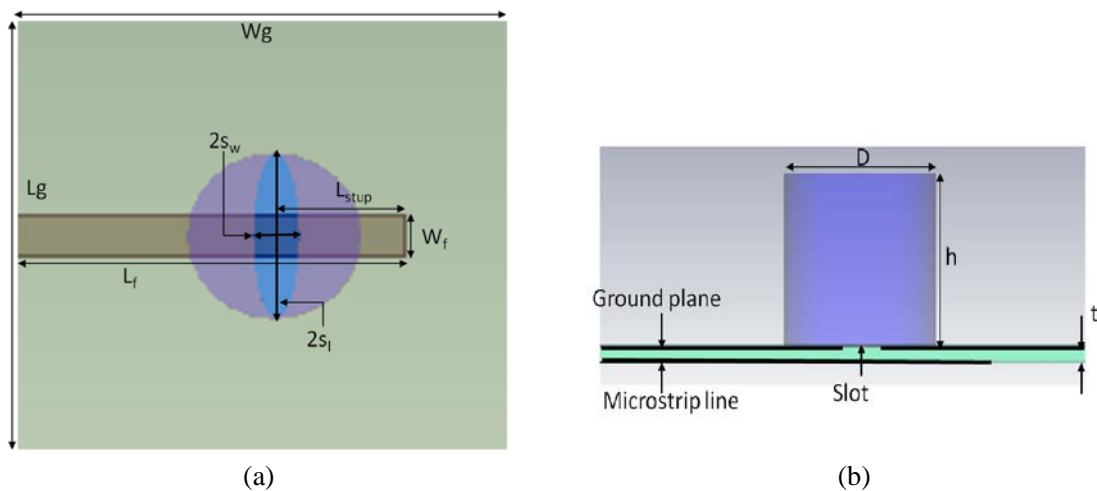
Figure 1. Elliptical slot cylindrical shape DRA; (a) Top view and (b) side view with design parameters.

The resonant frequency f_r of an isolated DR cylinder is calculated by [30]:

$$f_r = \frac{c}{2\pi a \sqrt{\varepsilon_{rdr}}} \left[1.71 + 2 \left(\frac{a}{2h} \right) + 0.1578 \left(\frac{a}{2h} \right)^2 \right] \tag{1}$$

Here $a = D/2$ (in cm), D and h are respectively the diameter and the height of each DR, ε_{rdr} the relative permittivity of the DR material, and c is the speed of light.

A parametric study was performed for the elliptical slot cylindrical DRA where one design parameter at a time was varied, while all other parameters were held constant. A parametric study of the proposed antenna was carried out using the Computer Simulation Technology (CST) microwave studio suite [29], an electromagnetic simulator based on the finite integration technique (FIT).

3. PARAMETRIC STUDY

The influence of various design parameters was investigated by the parametric approach. Figure 2 shows the reflection coefficient obtained from simulations of the DRA by varying the major slot radius (s_l) of DRA from 2.9 mm to 2.98 mm. Optimum impedance bandwidth was achieved at a major slot radius of 2.98 mm, where the slot size was approximately equal to the diameter of the DR.

Figure 3 shows the simulated reflection coefficient of the DRA, where varying the minor slot radius (s_w) leads to changes in the positions of the resonant frequencies and also the bandwidth. It is found that the matching condition of the slot-DR deteriorated with decreasing minor slot radius. However,
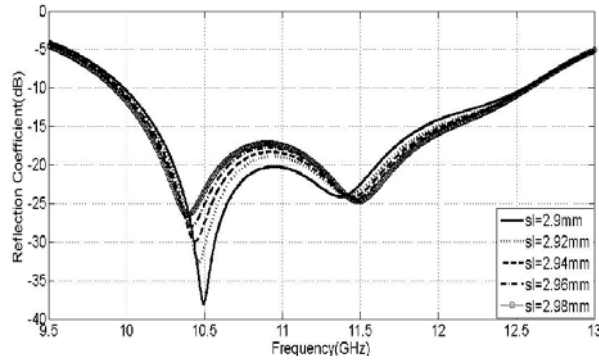
Figure 2. Comparison of reflection coefficient plots for various major slot radii s_l with $s_w = 0.75$ mm, and $l_l = 4$ mm.
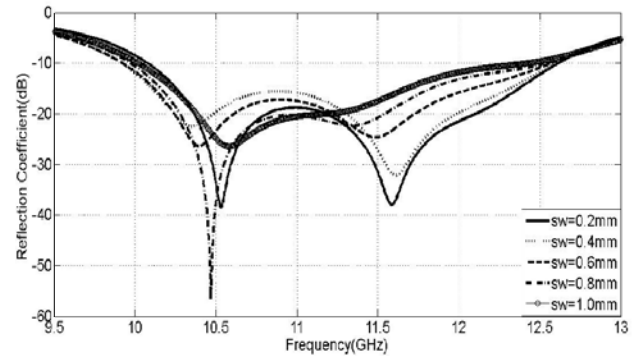
Figure 3. Comparison of reflection coefficient plots at various minor slot radii s_w, with $s_l = 2.98$ mm and $l_l = 4$.
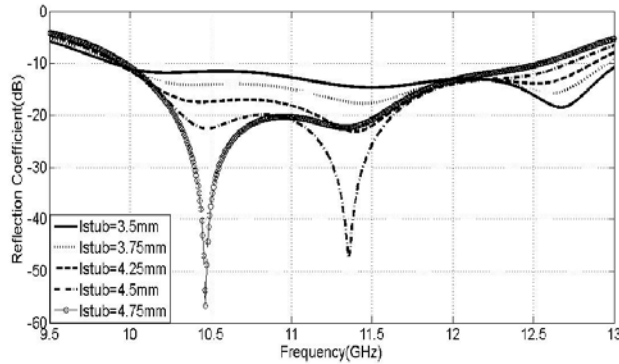
Figure 4. Comparison of reflection coefficient plots at various stub lengths l_l, with $s_l = 2.98$ mm and $s_w = 0.8$ mm.
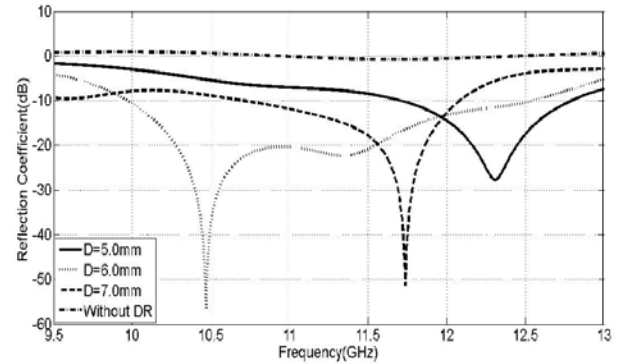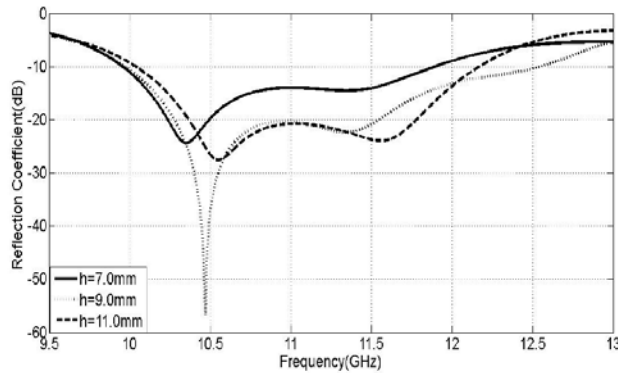
Figure 5. Comparison of reflection coefficient plots at various DR diameters D, at slot dimensions of $s_w = 0.8$ mm, $l_l = 4.5$ mm, and $s_l = 2.98$ mm.

since the back lobe of the radiation pattern will be enhanced due to increasing the minor slot radius, the minor slot radius should be chosen properly considering the matching bandwidth and acceptable back lobe level. The design was optimized at a minor slot radius of $s_w = 0.8$ mm.

Figure 4 shows the variation of the reflection coefficient as a function of frequency for various lengths l_l of the stub at the tip of the feed line. It can be seen that tuning the stub length greatly affected the matching and bandwidth of the antenna. The design was optimized at $l_l = 4.5$ mm.

Figure 5 shows the variation of the reflection coefficient as a function of frequency for different DRA diameters D. It can be seen that without the DR there was a high reflection as indicated by S_{11} approaching zero dB for the frequencies shown. The flat response indicates that the slot and stub parts of the antenna are far from resonance in the 9–15 GHz band under consideration With increasing diameter, the resonant frequency decreased and there was an increase in the impedance bandwidth. These results are in accordance with Eq. (1) which shows an overall inverse relation between the resonance frequency and the DR radius. For the DR used here, the resonance frequency according to Eq. (1) is 10.629 GHz. Figures 2 to 6 show dips in the obtained S_{11} responses around this frequency. Thus $D = 6$ mm was found to be the best value for the DR diameter for a slot major axis of 5.96 mm. This is in accordance with the conclusion drawn from the results in Figure 2 which showed that the best performance occurs when the diameters of the slot and the DR were approximately equal.

The variation of reflection coefficient with different DR heights is shown in Figure 6, where it is clear that larger height (h) results in a lower resonance frequency, such that the dip in S_{11} response moves towards the left. This finding is in accordance with Eq. (1). It can also be seen that a better impedance bandwidth with a minimum reflection coefficient loss was achieved at a height of $h = 9$ mm.

Figure 6. Comparison of reflection coefficient plots at different DR heights h.
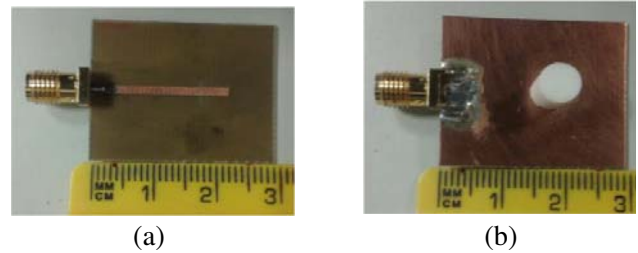
Figure 7. Photographs of the fabricated antenna, (a) back view and (b) front view.

4. THE OPTIMIZED DESIGN

According to the above parametric studies, the optimized design dimensions of the DRA are shown in Table 1. The proposed antenna was fabricated and tested. The fabricated antenna is shown in Figure 7.
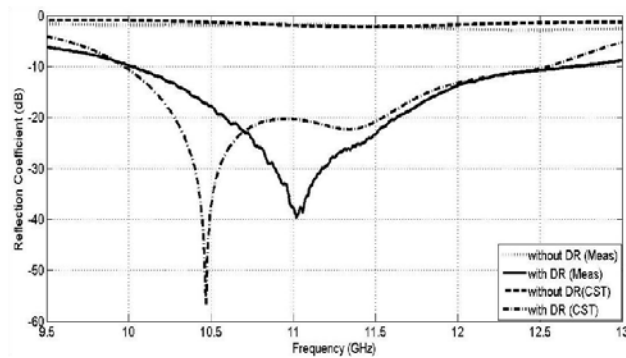
The reflection coefficient was measured using an HP (8510C) Vector Network Analyzer (VNA). Figure 8 compares the simulated and measured reflection coefficients, where it can be seen that the simulated antenna offers good matching for frequencies between 9.97 GHz and 12.558 GHz. A percentage bandwidth of 23% and a minimum reflection coefficient of about -56 dB at a frequency of 10.6 GHz were achieved. The fabricated antenna offered good matching for frequencies from 10.1 GHz to 12.7 GHz, a percentage bandwidth of 22%, with a minimum reflection coefficient achieved of about -40 dB at a frequency of 11 GHz. Thus the measured and simulated results agreed well, which helps to validate the design accuracy.

Figure 9 shows the simulated and measured gains of the proposed antenna as a function of frequency. It is noted from the figure that the realized gain varies between 7.23 dBi and 5.5 dBi across the operating

band from 9.97 to 12.558 GHz, with a maximum of 7.23 dBi at 10.6 GHz. For comparison, the gain was calculated for the case without the DR and plotted on the same figure, where it is seen that without the DR the antenna has very little gain across the band of interest. It should be noted here that the case without the DR was realized by simply removing the DR and keeping all dimensions the same, with no new optimization. Another conclusion is that a slot of such size is a poor radiator at the investigated frequencies unless it is coupled to an efficient radiating element such as the DR.

Table 1. Optimized parameters of the proposed antenna. All dimensions are in millimeters.

W_g	L_g	D	h	s_l	s_w	l_f	W_f	l_l
25	30	6	9	2.98	0.8	22.5	1.5	4.5

Figure 8. Simulated and measured reflection coefficients of the DRA.
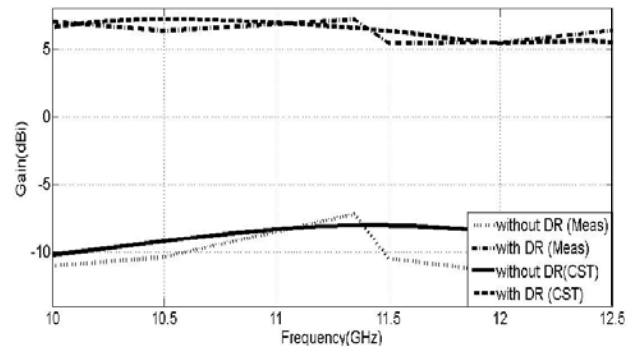
Figure 9. Simulated and measured gains versus frequency for the proposed DRA with and without a DR.
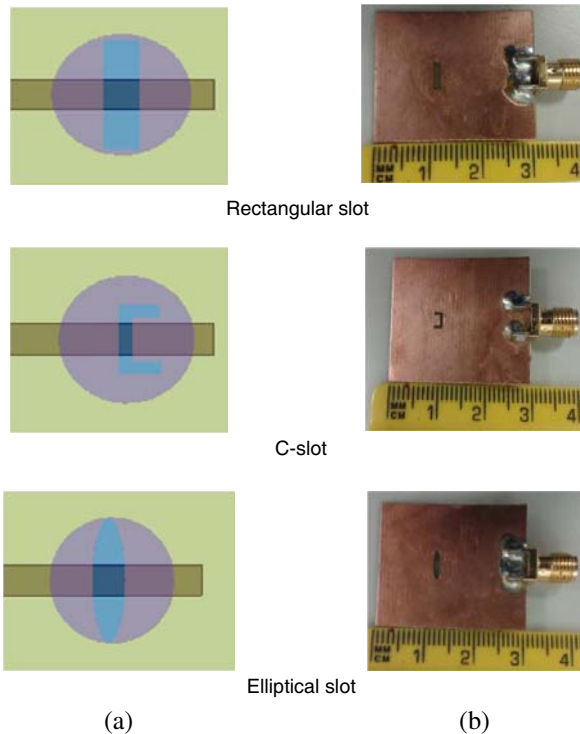

Figure 10. Investigated shapes of slots of DRAs: Simulated with CST, (b) fabricated antennas.

5. EFFECT OF SLOT SHAPE

In this section, the effect of the slot shape is discussed. Three shapes were considered: rectangle, C-shape and ellipse. The shape and size of the DRA were kept the same in these investigations. In order to compare the simulation results of the antennas, the proposed elliptical slot cylindrical DRA antenna, rectangular slot cylindrical DRA antenna and C-shaped slot cylindrical DRA antenna were manufactured and measured. The fabricated antennas are shown in Figure 10. The scattering parameters were measured by using an HP (8510C) VNA. The plots of simulated and measured reflection coefficients versus frequency for the fabricated DRAs with the three slot shapes are shown in Figure 11, where it is clear that the rectangular slot offered the largest impedance bandwidth. However, the elliptical slot gave a better compromise between bandwidth and matching. The obtained bandwidth with elliptical slot was from 9.97 GHz to 12.548 GHz.

The measured and simulated gain values are shown in Figure 12, showing that the shape of the slot made a slight difference in the gain bandwidth performance, and the elliptical slot gave the best response.
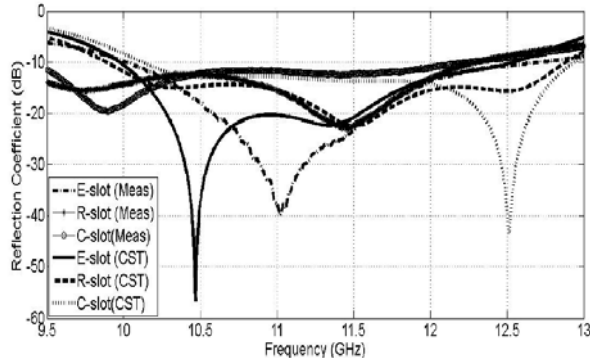
Figure 11. Simulated and measured reflection coefficient magnitude (S_{11}) versus frequency for the three proposed antennas.
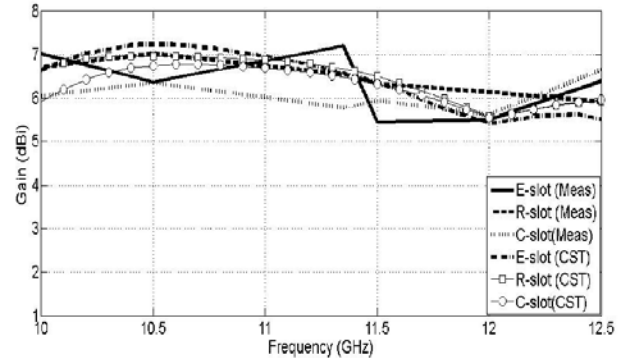
Figure 12. Simulated and measured gain (dBi) versus frequency for the three proposed antennas.

Figure 13 shows the normalized far-field radiation patterns at three frequencies, 10.5 GHz, 11.5 GHz and 12.5 GHz, for the three different slot shapes.

6. BAND NOTCHING

Band rejection can be achieved by implementing a U-shape slot in the feed line [26]. This slot represents a folded half-wavelength resonator with two short circuited ends. The U-slot is designed to resonate at the desired notch frequency. The geometry of the elliptical slot cylindrical shape DRA with a U-shaped slot in the feed line is shown in Figure 14. The slot was designed such that its average length (L_s) was equal to half the effective wavelength in the slot λ_e, where:

$$\lambda_e = \lambda_o / \sqrt{\varepsilon_{re}} \tag{2}$$

and ε_{re} is the effective relative dielectric constant of the substrate which is calculated as [31]:

$$\varepsilon_{re} = (\varepsilon_r + 1)/2 \tag{3}$$

Combining Eqs. (2) and (3), it can be shown the average slot length L_s can be given by:

$$L_s = 150/f\sqrt{\varepsilon_{re}} \tag{4}$$

where the slot length is in mm, and notched frequency is in GHz. The above formulas gave a very good estimate of the notch frequency; a more precise value can be tuned with the help of CST simulation. The parameters of this design and the simulated results for these antennas are shown in Table 2 and Figure 15. The last column of Table 2 compares the estimated slot length (L_s) and half the effective
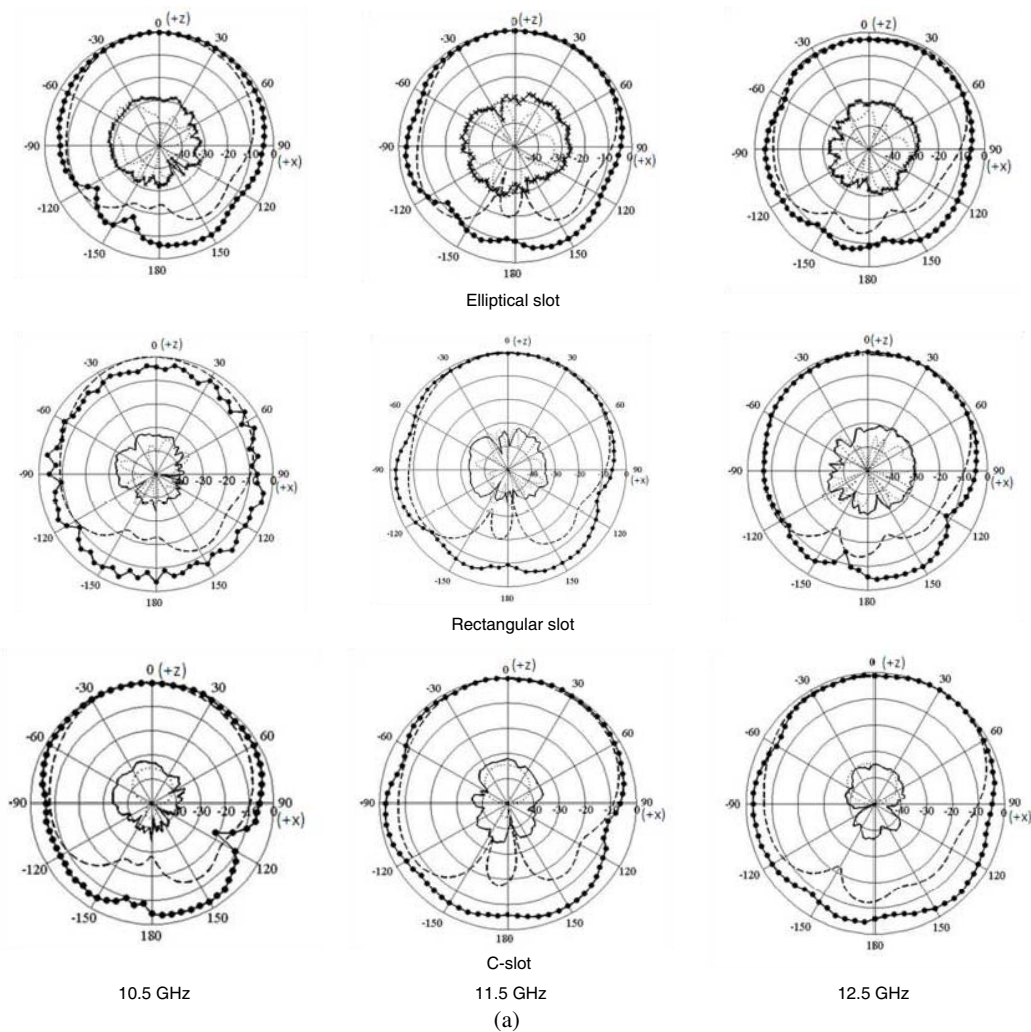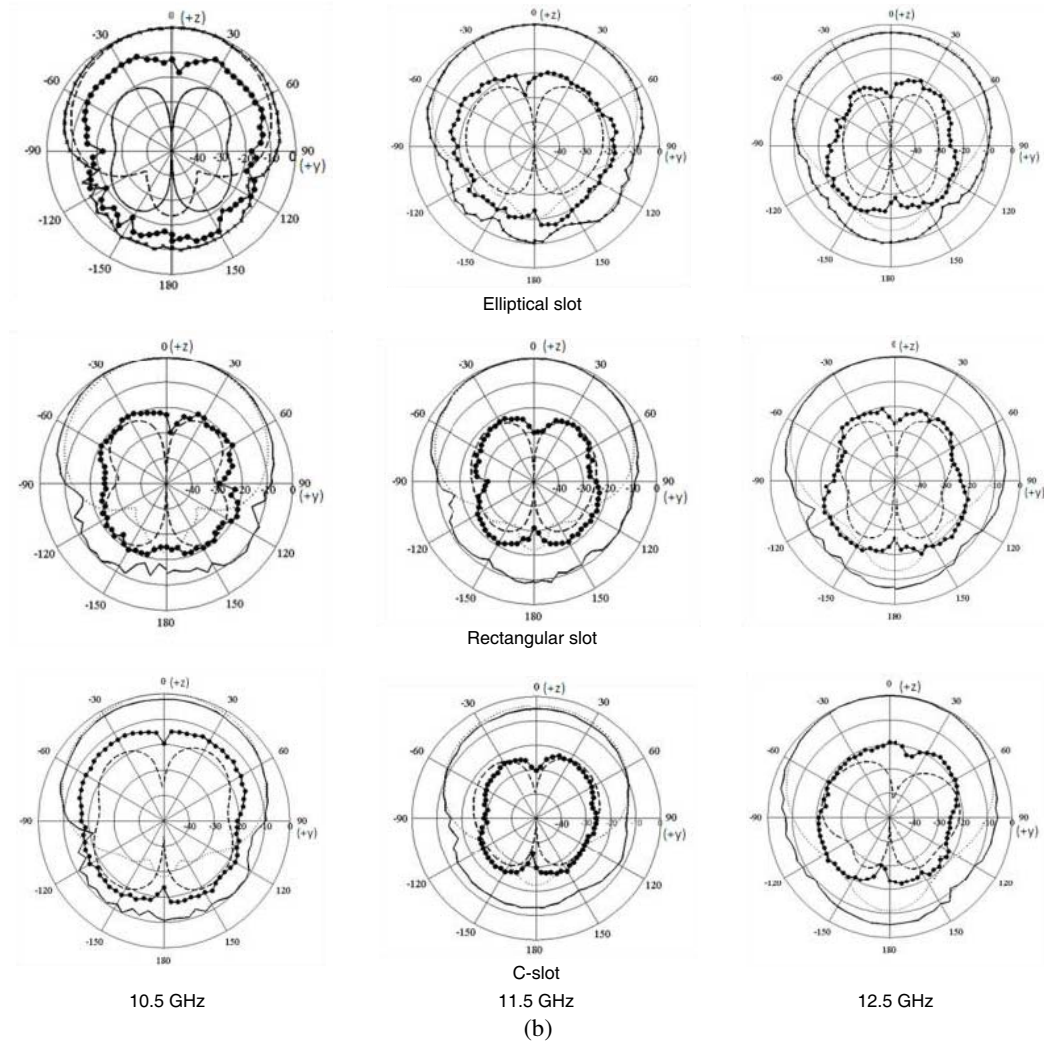
Table 2. Frequency characteristics from the results of Figure 15.

L_s (mm)	F_L–F_u (GHz)	F_n (GHz)	S_{11} (dB)	$L_s/(0.5\lambda_e)$
without slot	9.97–12.558	-	−54 dB at 10.47 GHz	-
8.9	10.832–11.472	11.08	−5.1	1.089
9.1	10.581–11.271	10.81	−5.09	1.087
9.3	10.37–10.967	10.57	−5.29	1.087
9.5	10.18–10.589	10.35	−5.44	1.087
9.7	9.993–10.397	10.16	−5.24	1.089

wavelength at the notch frequency (λ_{en}). This ratio should be unity if the prediction of Eq. (4) is exact; however, Table 2 shows that the deviation in prediction is 8.8% on average.

To adjust the notch-band frequency to the desired value without varying the width of the band, various values of slot length L_s were considered while the U-slot arms separation w_s was kept constant at 0.2 mm. The reflection coefficient characteristics obtained are shown in Figure 15. It is obvious that without a slot ($L_s = 0$), there was no notch behavior in the response. The notch frequency decreased with increasing slot length L_s. It was found that for a slot length of $L_s = 9.3$ mm, the notch frequency was 10.57 GHz. The reflection coefficient at this frequency was −5.29 dB, lower by 22.98 dB compared

Elliptical slot

Rectangular slot

C-slot

10.5 GHz   11.5 GHz   12.5 GHz

(a)

Figure 13. Normalized radiation pattern plots for different shapes of the slot of DRAs at 10.5 GHz, 11.5 GHz and 12.5 GHz) (a) xz plane and (b) yz plane.

Table 3. Frequency characteristics from the results of Figure 16.

| w_s (mm)	F_L–F_u (GHz)	F_n (GHz)	S_{11} (dB)
0.15	10.468–10.864	10.636	−6.22
0.2	10.369–10.973	10.57	−5.29
0.25	10.246–11.094	10.5	−4.07
0.3	10.151–11.199	10.445	−3.53

to the case before using the folded slot.

To explore the effect of the U-slot arm separation w_s, several values of w_s were considered while the length was kept constant at $L_s = 9.3$ mm. Results obtained are shown in Figure 16 and Table 3. It is clear that increasing the value of w_s improved the notch performance, where the reflection coefficient went up at the notch frequency, while the notch frequency was also slightly affected by varying the slot width.
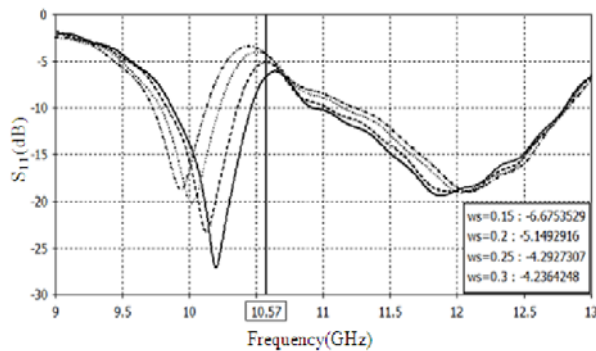
The band notch characteristic may not only be affected by the length and the arms separation
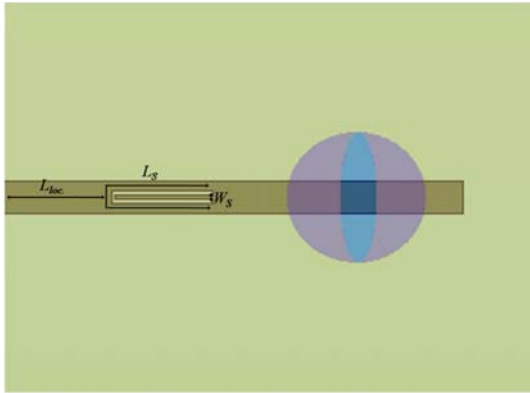
Figure 14. Antenna geometry showing the slot on the feed line and its parameters.
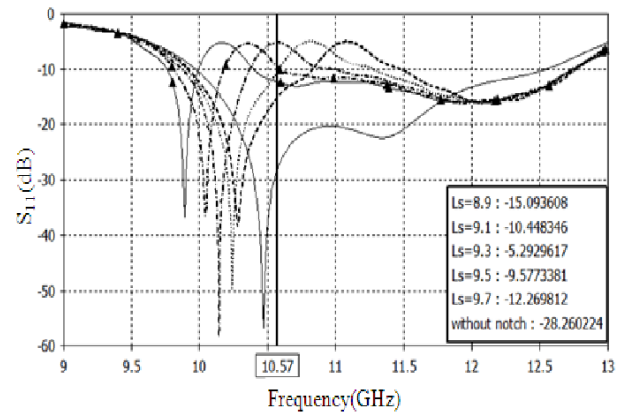
Figure 15. Variation of the reflection coefficient with frequency for various slot lengths L_s with $w_s = 0.2\,\text{mm}$, U-slot arms width of $0.15\,\text{mm}$ and $L_{loc} = 7.5\,\text{mm}$.

Figure 16. Variation of the reflection coefficient with frequency for various slot widths w_s with $L_s = 9.3\,\text{mm}$, U-slot arms width of $0.15\,\text{mm}$ and $L_{loc} = 7.5\,\text{mm}$.
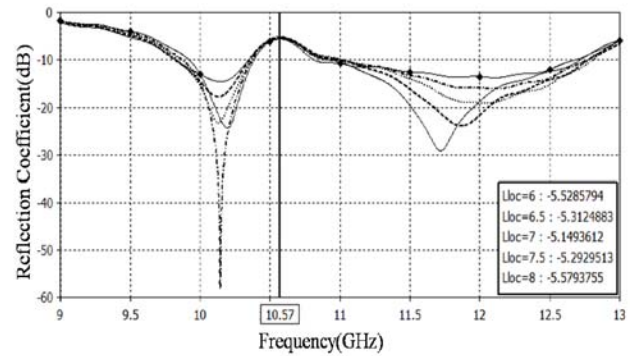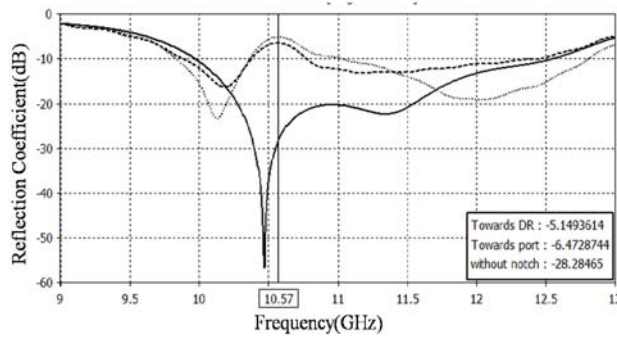

Figure 17. Variation of the reflection coefficient with frequency for various slot locations L_{loc} with $L_s = 9.3\,\text{mm}$, U-slot arms width of $0.15\,\text{mm}$ and $w_s = 0.2\,\text{mm}$.

of the U-slot but also by the location L_{loc} of the U-slot along the feed line. Different values of L_{loc} were considered in the investigation to illustrate this effect as demonstrated by the results shown in Figure 17. It is clear that changing the location of the slot had a noticeable effect on the reflection coefficient response before and after the notch frequency. The best response is obtained for $L_{loc} = 7\,\text{mm}$ from the feeding port.

The influence of the direction of the folded slot was also investigated, and the results obtained are shown in Figure 18, with better performance when the opening of the U-slot was directed towards the DR. The difference in the results for the two directions can be attributed to the distribution of the surface current along the feed line. Thus the antenna with the opening of a U-slot towards the DR was fabricated and tested for both reflection coefficient and gain. The fabricated antenna is shown in Figure 19.

The notch band characteristics are shown in Figure 20(a). Both the simulated and measured results show multiple resonances which were responsible for the wide bandwidth performance. The slight variation in the frequency range can be attributed to fabrication errors. Figure 20(b) shows the simulated and measured realized gain variation with frequency of the proposed antenna without notch and with notch (the opening of the U-slot was directed towards the DR). It is noted from the figure that with the U-slot added to the antenna, the realized gain at the notch frequency decreased to a value

Figure 18. Variation of the reflection coefficient with frequency for two directions of the folded slot and for no notch; without notch (solid), towards DR (dotted) and towards port (dashed).
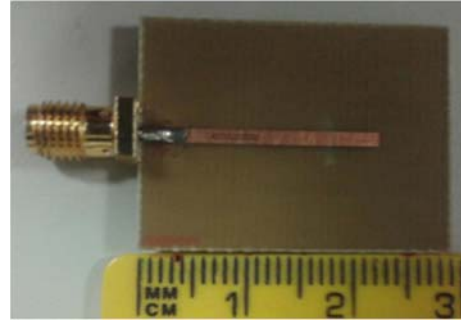
Figure 19. Photograph of the fabricated elliptical slot antenna with the addition of a U-slot.
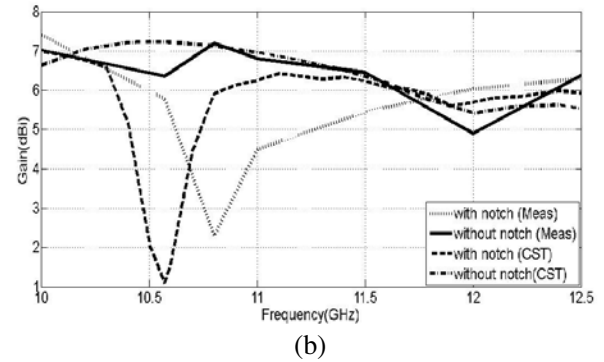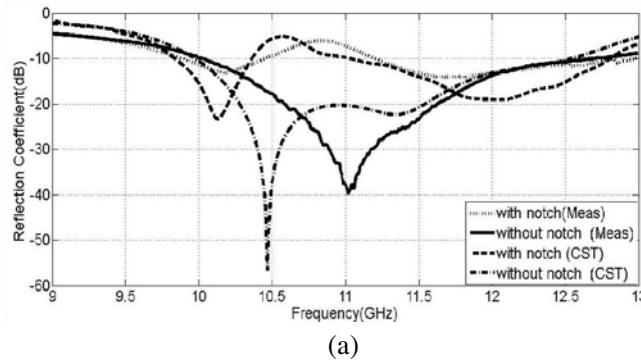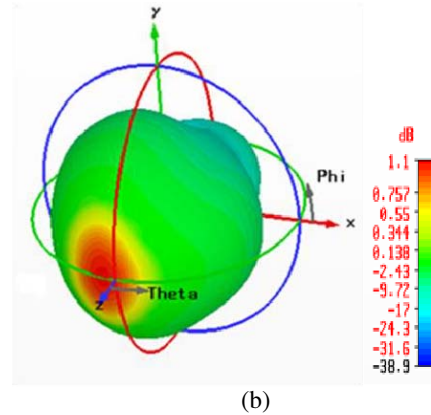

Figure 20. Simulated and measured (a) reflection coefficient and (b) gain versus frequency of the proposed DRA with and without notch.
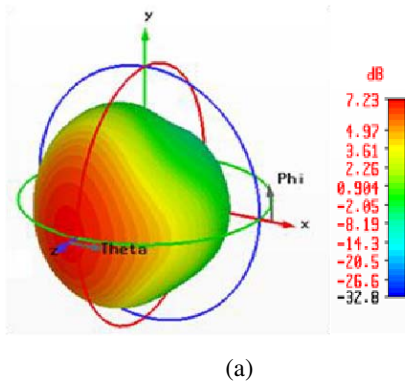
Figure 21. Simulated 3D radiation patterns of the proposed DRA at 10.57 GHz (a) without notch and (b) with notch.

of 1.10 dBi which means that a reduction in gain of 6.13 dB was achieved by notching.

Figure 21 shows the three dimensional far-field radiation patterns for the proposed antenna with and without a notch (again note that the opening of the U-slot was directed towards the DR) at 10.57 GHz. It can be seen that the radiation efficiency of the antenna without the U-slot was 98.88%. By adding the U-slot to the antenna the radiation efficiency went down to 36.79% at the notch frequency, a reduction

in radiation efficiency of 62.09%. Therefore, the good performance of the notching slot was ascertained by a decrease of 22.98 dB in the reflection coefficient, a reduction in gain of 6.13 dB in gain, as well as a reduction in efficiency down to 36.79%.

7. CONCLUSIONS

A compact dielectric resonator antenna (DRA) with band-notched characteristics for UWB applications has been demonstrated. The proposed design is a result of comprehensive parametric study using CST Microwave Studio suite$^{\text{TM}}$ 2011. The investigations showed the effect of various parameters of the antenna on the resulting performance. Simulation results show that the proposed DRA has a -10 dB impedance bandwidth of 23% from 9.97 GHz to 12.558 GHz, and a maximum gain of 7.23 dBi. The antenna had a notched band centered at 10.57 GHz with a reflection coefficient of -5.149 dB: the realized gain decreased by 6.13 dB to the value of 1.10 dBi at the notch frequency. The optimized designs were verified by experimental measurements on the fabricated samples.

REFERENCES

1. Petosa, A., A. Ittipiboon, Y. M. M. Antar, D. Roscoe, and M. Cuhaci, "Recent advances in dielectric-resonator antenna technology," *IEEE Antennas and Propagation Magazine*, Vol. 40, No. 3, 35–48, 1998.

2. Lee, M. T., K. M. Luk, E. K. N. Yung, and K. W. Leung, "Microstrip-line feed circularly polarized cylindrical dielectric resonator antenna," *Microwaves and Optical Technology Letters*, Vol. 24, No. 3, 206–207, 2000.

3. Menon, S. K., et al, "Wideband cylindrical dielectric resonator antenna excited using an L-strip feed," *Microwaves and Optical Technology Letters*, Vol. 42, No. 4, 293–294, 2004.

4. Song, Y. and A. R. Sebak, "Radiation pattern of aperture coupled prolate hemispheroidal dielectric resonator antenna," *Progress In Electromagnetics Research*, Vol. 58, 115–133, 2006.

5. Albooyeh, M., N. Komjani, and M. Shobeyri, "A novel cross-slot geometry to improve impedance bandwidth of microstrip antennas," *Progress In Electromagnetics Research Letters*, Vol. 4, 63–72, 2008.

6. Thamae, L. Z. and W. Zhipeng, "Broadband bowtie dielectric resonator antenna," *IEEE Transactions on Antennas and Propagation*, Vol. 58, No. 11, 3707–3710, 2010.

7. Zou, L., D. Abbot, and C. Fumeaux, "Omnidirectional cylindrical dielectric resonator antenna with dual polarization," *IEEE Antennas and Wireless Propagation Letters*, Vol. 11, 515–518, 2012.

8. Mehak, G. and S. K. Sharma, "Wide-bandwidth dielectric resonator antenna with omni-directional radiation patterns for beam focusing properties in a circular array," *International Journal of RF and Microwave Computer-Aided Engineering*, Vol. 24, No. 1, 92–101, 2014.

9. Mongia, R. K. and P. Bhartia, "Dielectric resonator antennas — A review and general design relations for resonant frequency and bandwidth," *International Journal of Microwave and Millimeter-Wave Computer-Aided Engineering*, Vol. 4, No. 3, 230–247, 1994.

10. Fang, X. S. and K. W. Leung, "Designs of single-, dual-, wide-band rectangular dielectric resonator antennas," *IEEE Transactions on Antennas and Propagation*, Vol. 59, No. 6, 2049–2014, Jun. 2011.

11. Pan, Y. M. and K. W. Leung, "Wideband omnidirectional circularly polarized resonator antenna with parasitic strips," *IEEE Transactions on Antennas and Propagation*, Vol. 60, No. 6, 2992–2997, 2012.

12. Maknikar, R. D. and V. G. Kasabegoudar, "Circularly polarized cross-slot-coupled stacked dielectric resonator antenna for wireless applications," *International Journal of Wireless Communications and Mobile Computing*, Vol. 1, 68–73, 2013.

13. Majeed, A. H., A. S. Abdullah, F. Elmegri, K. H. Sayidmarie, R. A. Abd-Alhameed, and J. M. Noras, "Aperture-coupled asymmetric dielectric resonators antenna for wideband applications," *IEEE Antennas and Wireless Propagation Letters*, Vol. 13, 927–930, 2014.

14. Mudavath, S., R. Kumari, and S. K. Behera, "A compact CPW fed stacked cylindrical dielectric resonator antenna for WLAN applications," *The 2012 International Conference on Computing, Electronics and Electrical Technologies (ICCEET)*, 818–820, Kumaracoil, Mar. 21–22, 2012.

15. Elmegri, F., C. H. See, R. A. Abd-Alhameed, C. Zebiri, and P. S. Excell, "Dielectric resonator antenna design for UWB applications," *The 2013 Loughborough Conference on Antennas and Propagations (LAPC)*, 539–542, Loughborough, Nov. 11–12, 2013.

16. Wang, Y. F., T. A. Denidni, Q. S. Zeng, and G. Wei, "Band-notched UWB rectangular dielectric resonator antenna," *Electronics Letters*, Vol. 50, No. 7, 483–484, 2014.

17. Liu, Y., M. Wei, H. Liu, and S. Gong, "A novel compact three-port dielectric resonator antenna with reconfigurable pattern for WLAN systems," *Progress In Electromagnetics Research C*, Vol. 47, 37–45, 2014.

18. Petosa, A., *Dielectric Resonator Antenna Handbook*, Artech House Publishers, 2007.

19. Lee, W. S., D. Z. Kim, K. J. Kim, and J. W. Yu, "Wide-band planar monopole antennas with dual band-notched characteristics," *IEEE Transactions on Microwave Theory & Techniques*, Vol. 54, No. 3, 2800–2806, 2008.

20. Li, Y. S., X. D. Yang, C. Y. Liu, and T. Jiang, "Compact CPW-fed ultrawideband antenna with dual band-notched characteristics," *Electronics Letters*, Vol. 46, No. 14, 967–968, 2010.

21. Jiang, J. B., Z. H. Yan, and J. Y. Zhang, "Dual band-notched ultra-wideband printed antenna with two different typed slots," *Microwave and Optical Technology Letters*, Vol. 52, No. 9, 1930–1933, 2010.

22. Chu, Q.-X. and T.-G. Huang, "Compact UWB antenna with sharp band-notched characteristics for lower WLAN band," *Electronics Letters*, Vol. 47, No. 15, 838–839, 2011.

23. Nguyen, D. T., D. H. Lee, and H. C. Park, "Very compact printed triple band-notched UWB antenna with quarter-wavelength slots," *IEEE Antennas and Wireless Propagation Letters*, Vol. 11, 411–414, 2012.

24. Wang, J. W., J. Y. Pan, X. N. Xiao, and Y. Q. Sun, "A band-notched UWB antenna with L-shaped slots and open-loop resonator," *The 2013 IEEE International Conference on Applied Superconductivity and Electromagnetic Devices (ASEMD)*, 312–315, Beijing, Oct. 25–27, 2013.

25. Zhang, C., J. Zhang, and L. Li, "Triple band-notched UWB antenna based on SIR-DGS and fork-shaped stubs," *Electronics Letters*, Vol. 50, No. 2, 67–69, 2014.

26. Sayidmarie, K. H. and T. A. Najm, "Performance evaluation of band notch techniques for printed dual band monopole antennas," *International Journal of Electromagnetics and Applications*, Vol. 3, No. 4, 70–80, 2013.

27. Jahanbakht, M. and A. A. L. Neyestanak, "A survey on recent approaches in the design of band notching UWB antennas," *Journal of Electromagnetic Analysis and Applications*, Vol. 4, 77–84, 2012.

28. Zhu, F., S. Gao, A. T. Ho, R. Abd-Alhameed, C. H. See, T. W. C. Brown, J. Li, G. Wei, and J. Xu, "Multiple band-notched UWB antenna with band-rejected elements integrated in the feed line," *IEEE Transactions on Antennas and Propagation*, Vol. 61, No. 8, 3952–3960, 2013.

29. "CST: Computer simulation technology based on FIT method," CST Computer Simulation Technology AG, 2011.

30. Kishk, A., et al., "Slot excitation of the dielectric disk radiator," *IEEE Transactions on Antennas and Propagations*, Vol. 43, No. 2, 198–201, Feb. 1995.

31. Ren, L.-S., F. Li, J.-J. Zhao, G. Zhao, and Y.-C. Jiao, "Compact printed ultra wideband monopole antenna with dual band-notched characteristics," *Journal of Electromagnetics Waves and Applications*, Vol. 24, 1521–1529, 2010.